

Combustion characteristics of a swirl chamber type diesel engine[†]

Gyeong Ho Choi¹, Jae Cheon Lee², Tae Yun Kwon³, Chang Uk Ha⁴, Jong Soon Lee⁴,
Yon Jong Chung⁵, Yong Hoon Chang⁶ and Sung Bin Han^{6,*}

¹*EROOM G & G Co., Ltd., 83-1 Nakha-ri, Tanhyeon-myeon, Paju-si, Gyeonggi-do, 413-843, Korea*

²*Department of Mechanical & Automotive Engineering, Keimyung University, Daegu, 704-701, Korea*

³*Graduate School of Automotive Engineering, Keimyung University, Daegu, 704-701, Korea*

⁴*Daedong Co., Ltd., R & D Center, Changnyung-gun, Gyeongnam, 635-806, Korea*

⁵*Department of Automotive Engineering, Daegu Mirae College, Gyeongsan-si, Gyeongbuk, 712-716, Korea*

⁶*Department of Mechanical & Automotive Engineering, Induk University, San 76 Wolgye-dong, Nowon-gu, Seoul, 139-749, Korea*

(Manuscript Received June 24, 2008; Revised June 30, 2009; Accepted August 9, 2009)

Abstract

A numerical model that utilizes Computational Fluid Dynamics (CFD) techniques is simulated for the analysis of a swirl chamber type diesel engine. This research also reveals the effects of swirl chamber passage hole geometry on the combustion characteristics of a swirl chamber type diesel engine depending on the shape, angle, and area of the jet passage. Turbulence kinetic energy is generated by compound effects of the pressure, heat release, NOx concentrations, and soot concentrations. Results show that combustion characteristics are affected by the passage hole areas and the passage hole inclination angles.

Keywords: Heat release rate; NOx; Swirl chamber; Soot concentrations; Turbulence

1. Introduction

Diesel-powered vehicles are popular for heavy-load transportation because their fuel efficiency is higher than that of gasoline-powered vehicles. Although diesel engines provide convenience in daily life, they produce foul-smelling emissions that contain many types of toxic air pollutants, including hydrocarbon, carbon monoxide, nitrogen oxides, sulfur oxides, volatile organic compounds, semi-volatile organic compounds, and soot. To improve air quality, diesel engines are thus subject to severe emission regulations. These worldwide regulations have placed limitations on design modifications of diesel engines [1-3].

Nitrogen oxide (NOx) and particulate matter (PM) emissions of diesel vehicles are regarded as sources

of air pollution, and a global trend to enforce more stringent regulations on these exhaust gas constituents began in the early years of the 21st century. On the other hand, the excellent thermal efficiency of diesel engines is a welcome attribute from the standpoint of conserving energy and curbing global warming [4].

To simultaneously realize reduction in harmful emissions and improvement in fuel consumption of the swirl chamber type diesel engine, reduction of the mixture formation period and complete combustion must be pursued. Therefore, an optimum combustion chamber to achieve these tasks must first be designed. Theoretical and semi-experimental methods exist for the design of the swirl type combustion chamber, but the aberrations are too great. The currently used design method is mainly to optimize the process using a trial and error method based on accumulated knowledge [5-7].

In a swirl chamber type diesel engine, a strong swirl is produced inside the swirl chamber upstream

[†] This paper was recommended for publication in revised form by Associate Editor Kyoung Doug Min

*Corresponding author. Tel.: +82 2 950 7545, Fax.: +82 2 950 7559

E-mail address: sungbinhan@induk.ac.kr

© KSME & Springer 2009

of the combustion chamber during the compression stroke. By spraying the fuel into this chamber and forming a good mixture, the engine can obtain excellent combustion, even at high speeds. Swirl chamber type diesel engines are favorable for high-speed operations, and because, while small in size, they can produce high power, they are often used for small, high-speed diesel engine applications [8-9]. NOx generation is reduced in modern engines with fast-burn combustion chambers. The amount of NOx generated also depends on the location within the combustion chamber. Because they generally have higher compression ratios as well as higher temperatures and pressure, compression ignition (CI) engines with a divided combustion chamber and indirect injection (IDI) tend to generate higher levels of NOx [10].

Due to rapid advancement in computer hardware and the development of effective numerical modeling software, computer analysis using computational fluid dynamics (CFD) can quickly provide accurate information and complement existing research.

In this study, the effects of the area and the angle of the passage hole, which in earlier studies have been investigated and proven to be the primary design factors of the swirl chamber type diesel engine, were investigated. The combustion model used for the CFD simulation was based on the Lagrangian method. The Ricardo Two-Zone Flamelet (RTZF) model and the Zeldovich NOx production mechanisms were used [11, 12]. Through the commercial numerical analysis program VECTIS, the passage hole area and angle are varied for analysis of the expansion and exhaust stages. Through this method, we hope to provide background knowledge for the design of the optimum combustion chamber shape.

This paper aims to clarify the combustion characteristics in a swirl chamber-type diesel engine.

2. Numerical analysis

2.1 Analysis model

The main specifications and testing conditions of the engine are shown in Table 1. In Fig. 1, the shapes of the engine's swirl chamber and passage hole are presented. In order to investigate the effects of the passage hole area and angle — the main design factors of the swirl chamber-type diesel engine — on the turbulent flow and turbulent combustion of the engine, the two elements were varied, as shown in Table 2, for use in the analysis model. With Case 1, which has

Table 1. Engine specification.

Combustion System	Swirl Pre-combustion
Bore (mm)	87
Stroke (mm)	102.4
Con. Rod Length (mm)	133
Compression Ratio	21
Engine Speed (rpm)	1700
SOI (CA)	-18 deg. ATDC
Injection Mass (mg/cycle)	33.865

Table 2. Details of various conditions.

	VR	CR	θ (deg.)	A (mm ²)	D (mm)
Case 1	54.3	21.0	35	64.90	5.1
Case 2	54.1	21.1	35	49.51	4.1
Case 3	54.6	20.8	35	81.96	6.1
Case 4	54.4	20.9	30	64.90	5.1
Case 5	54.7	20.8	40	64.90	5.1

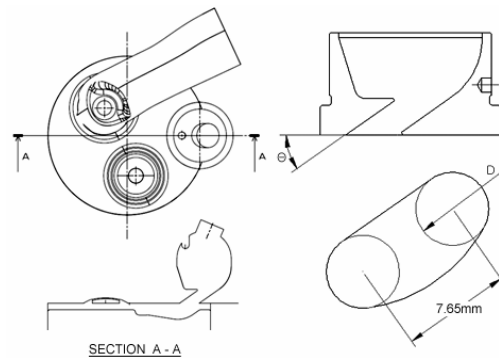


Fig. 1. Swirl chamber and jet passage shape.

a passage hole angle of 35° and an area of 64.9 mm^2 , serving as the reference, Case 2 and Case 3 were varied in regard to the area of the passage hole, and Case 4 and Case 5 were varied in regard to the angle of the passage hole.

2.2 Mesh generation

We used the VECTIS program to perform the numerical analysis. The mesh was generated directly from an STL file, which was compatible with the CAD model and the general-purpose FE preprocessor model. The mesh was created to be very fine near the boundaries to precisely define the surface, and block refinement was applied to the passage hole and swirl chamber areas to create fine-grid regions. By adding

the motions of the valve and the piston, a moving grid is set on the upper part of the valve and the piston.

The computational mesh for the engine is shown in Fig. 2. Since the analysis was performed on the top dead center of the compression process, the exhaust port and valve were excluded. After the intake valve was closed, the mesh was generated with the intake port and the intake valve excluded. The number of mesh cells generated at the top dead center of the compression process was approximately 134,000, and approximately 275,000 at the bottom center of the exhaust process.

2.3 Computational fluid dynamics (CFD) simulation

Three-dimensional unsteady CFD analysis was calculated using the mass conservation equation, momentum conservation equation, and energy conservation equation. When flow was turbulent, particles experienced random fluctuation in motion, superimposed on their main bulk velocity. A number of different models for turbulence, used in predicting flow characteristics, can be found in fluid mechanics literature. Turbulence is generated, diffused, and dissipated by the flow field, and the rate of change of k turbulent

kinetic energy and ϵ the dissipation rate of k should be considered with regard to the combustion chamber. In this study, the k - ϵ turbulent model was used to represent the turbulence phenomenon [13].

The combustion model used for the CFD simulation was based on the Lagrangian method. The RTZF model and the Zeldovich NO_x production mechanisms were used.

Fig. 3 shows the schematic representation of the two-zone model that assumes a burned zone and an unburned zone. The unburned zone is divided into two regions: segregated and mixed. In this study, the mixed region is assumed to mix with air and fuel fractions, and is used to prepare the chemical reactions.

The turbulence kinetic energy inside the swirl chamber at the end of the compression process is an important factor that influences the mixture of the fuel and air, and the flame propagation. Fig. 4 indicates the average turbulence kinetic energy for varying crank angles, and Fig. 5 presents the velocity vector cutting through the swirl chamber at CA 340°.

Turbulence kinetic energy increases until it reached around CA 100°, when valve lift is the greatest, and then decreases. It rises again while compression takes

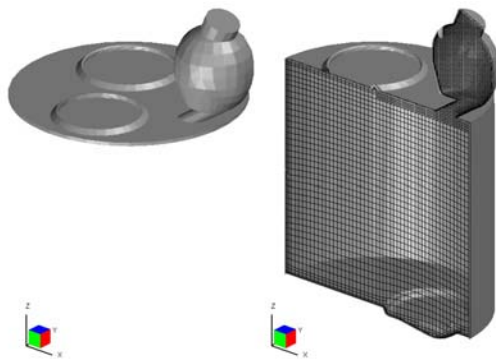


Fig. 2. CFD surface geometry and computational mesh.

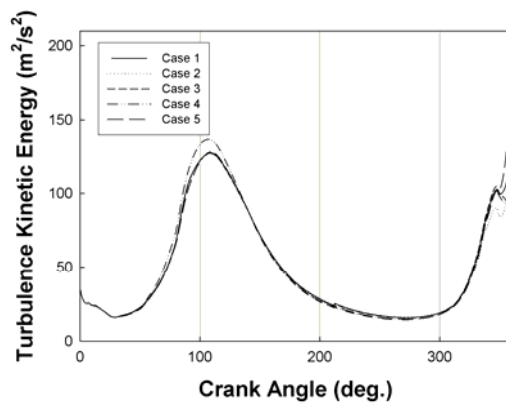


Fig. 3. Variations in turbulence kinetic energy with crank angle in various cases.

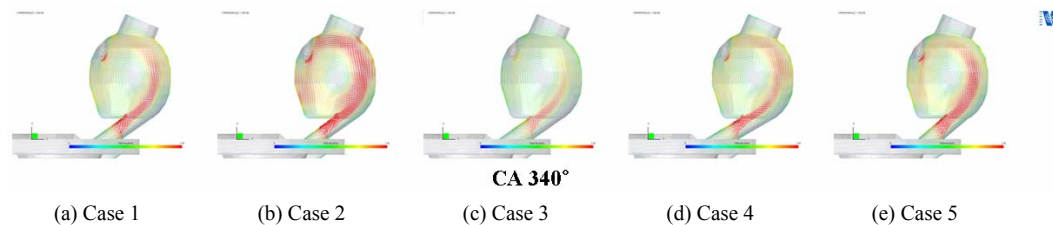


Fig. 4. Velocity vector in plan cutting through swirl chamber (CA 340 deg.).

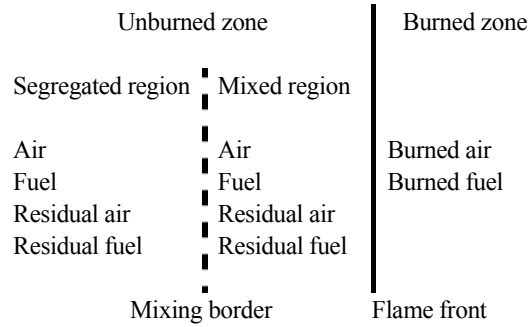


Fig. 5. Two-zone representation.

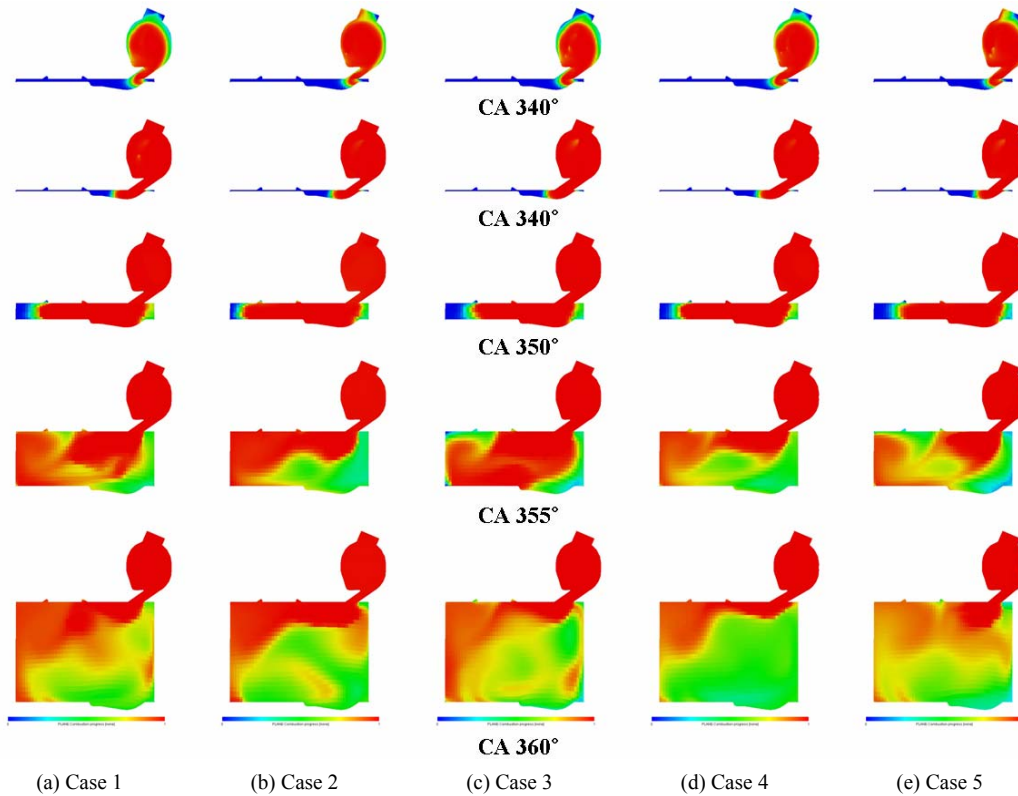


Fig. 6. Comparison of contour plots for combustion progress during the expansion process.

place. Case 4, at CA 100°, is approximately 5% larger compared to the other cases. It is believed that for Case 4, with its small passage hole inclination angle, part of the flow advancing towards the wall of the cylinder flows into the passage hole as the valve lift increases creates turbulence. Turbulence kinetic energy at CA 350° decreases once flow into the swirl chamber is completed and turbulence near the passage hole weakens.

3. Results and discussions

3.1 Combustion pressure and heat release

Fig. 6 demonstrates the comparison of contour plots for the combustion progress during the expansion process. In this figure, Case 2, with the smallest passage hole area of 49.51 mm², and Case 4, with the smallest passage hole angle of 30°, demonstrate rapid speed in the combustion process; however, the combustion at the end of the compression process leans

toward the left. Case 3, with the largest passage hole area, and Case 5, with the greatest passage hole angle, show slower speed in the combustion process than those of the other cases. Case 2, with the smallest passage hole area, demonstrates fast-burn combustion, with the combustion figure slanting to the left because of the inertia force.

It is believed that for Case 4, with its small passage hole inclination angle, the flame angle advancing towards the wall of the cylinder slants to the left.

For Case 3, which has the largest passage hole area, burning velocity is slow during the compression process because of turbulent flow velocity. For Case 5, it is believed that, due to its high passage hole inclination angle, the flame propagates close to the direction of the cylinder. The combustion process is also slow because the burning velocity is slow at the wall of the combustion chamber.

Fig. 7 indicates the variations in cylinder pressure with crank angle in various cases. The pressure rises to CA 347° after the fuel injection starts at CA 342°, and reaches the maximum pressure value at CA 362°. The maximum pressure value of Case 3, with the largest passage hole area, is smaller compared to the other cases, and the decrease in pressure occurs early in Case 5.

Figs. 8 and 9 show the variations in the heat release rate profile and variations in total heat release with crank angle in various cases, respectively. Here, Case 1, Case 4, and Case 5 demonstrate similarities in maximum value of heat release. Case 2, with the largest passage hole area, and Case 3 show smaller values in maximum heat release compared to the other cases. It is believed that for Case 2, the least turbulence in kinetic energy occurs around the maximum value of heat release at CA 348°, compared to the other cases. For Case 3, the least flow velocity occurs inside the cylinder.

In Case 2, with the smallest passage hole area, there is a small decrease of heat release rate before the start of diffusion combustion. It is believed that flame propagation in the main combustion chamber is difficult because of the narrow passage hole, and then the pressure descent is small and rich combustion continues to take place. In addition, Case 2 and Case 5 are no longer compared to the other cases in the period of heat release in the main combustion chamber. This is believed to be the reason for the pressure of the swirl chamber being comparatively high, and the flame propagation velocity being fast due to the narrow passage hole.

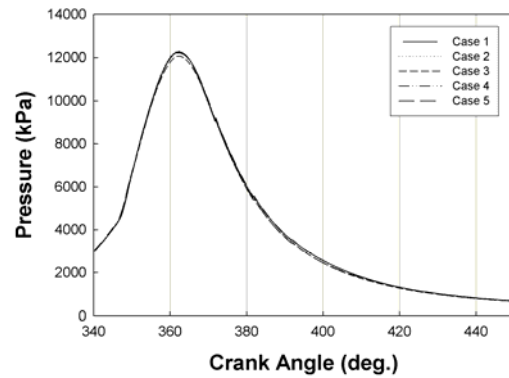


Fig. 7. Variations in cylinder pressure with crank angle in various cases.

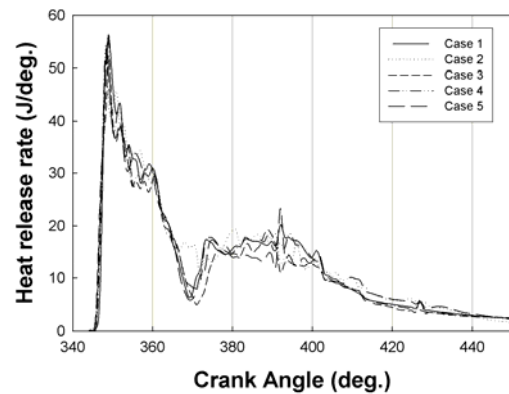


Fig. 8. Variations in heat release rate profile with crank angle in various cases.

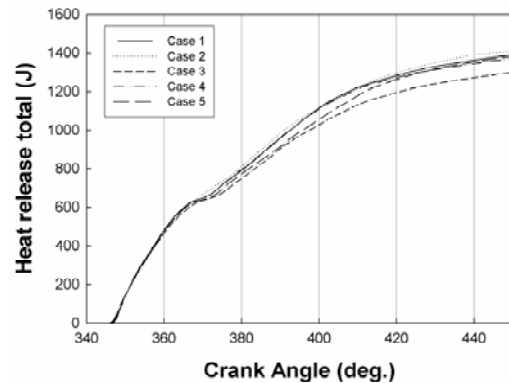


Fig. 9. Variations in total heat release with crank angle in various cases.

In Case 3 with the greatest passage hole area, the heat release rate during the diffusion combustion process begins late, compared to the other cases, and the heat release period is shorter.

The inclination angles of 30° (Case 1) and 35° (Case 4) result in similar the heat releases according to the passage hole inclination angles. However, the diffusion combustion of the inclination angle of 40° (Case 5) starts later than the others, and the heat release rate shows itself to be comparatively small; combustion period is extensive during the combustion process.

3.2 NOx and soot concentrations

Fig. 10 shows the NOx concentrations with crank angle in various cases. Table 3 shows the determination of air–fuel ratios. The NOx concentrations rapidly increase during the start of combustion and during the initial combustion stage; thus, the production of concentrations is almost completed at CA 25°. Here, the concentrations of Case 3 and Case 4 are the largest, followed by Case 1, Case 2, and Case 5, in that order.

In Case 2, there is a small decrease in heat release rate before the start of diffusion combustion. It is believed that the flame propagation in the main combustion chamber is difficult because of the narrow passage hole and an excess of oxygen that can combine with the nitrogen to form various oxides.

Table 3. Determination of air–fuel ratios.

	Air flow weight, kg/cycle	Fuel flow weight, kg/cycle	Air–fuel ratio
Case 1	0.000656723	0.000033865	19.392
Case 2	0.000655792	0.000033865	19.365
Case 3	0.000656803	0.000033865	19.395
Case 4	0.000660918	0.000033865	19.516
Case 5	0.000655651	0.000033865	19.361

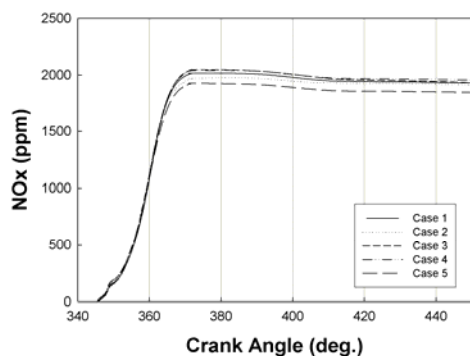


Fig. 10. NOx concentrations with crank angle in various cases.

Based on the passage hole angles, the NOx concentration is highest in Case 4, where the passage hole inclination angle is 30°. Case 5, with a passage hole inclination angle of 40°, shows the lowest. The flame propagation angle is considered to be the axle direction due to its large its passage hole inclination. As for the passage hole inclination angle, it is believed that NOx is affected by the difference in burning velocity in the main combustion chamber due to the flame propagation angle.

The formation of NOx depends on pressure, air–fuel ratio, and combustion time within the cylinder, with chemical reactions not being instantaneous. NOx is reduced in modern engines with fast-burn combustion chambers. The amount of NOx generated also depends on the location within the combustion chamber. The highest concentration is formed around the spark plug, where the highest temperature and pressure are located. Because they generally have higher compression ratios (see the CR of Table 2) and higher temperatures and pressure, compression ignition engines with divided combustion chamber and indirect injection (IDI) tend to generate higher levels of NOx [14].

Fig. 11 indicates the soot concentrations with angle in various cases. The values of soot concentrations slowly increase after the beginning of combustion and rapidly increase after CA 365°, when the decrease of pressure begins. They slowly decrease after CA 385°, when the maximum value is reached.

In Case 2, soot concentrations rapidly increase in the swirl chamber because of insufficient supply of oxygen compared to the other cases. Soot shows the lowest concentrations in Case 3, owing to the large passage hole area, which causes slow turbulence flow velocity and burning velocity in the swirl chamber.

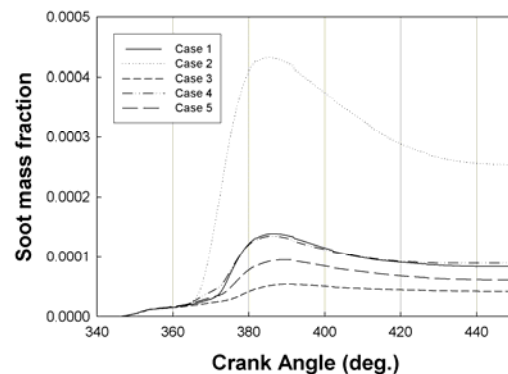


Fig. 11. Soot concentrations with crank angle in various cases.

Particulate generation can be reduced by engine design and control of operating conditions. Quite often, however, this will create other adverse results. If combustion time is extended by the combustion chamber design and timing control, particulate amounts in the exhaust can be reduced. Soot particles originally generated will take a longer time to mix with oxygen and be combusted to CO₂ (see the passage hole area (A) of Table 2). However, a longer combustion time means a high cylinder temperature and more NO_x generated [14]. In the soot concentrations according to the passage hole angles, Case 4 (30°) shows close similarity to Case 1 (35°). Case 5 (40°) shows the lowest soot concentrations.

4. Conclusion

This study aims to clarify the combustion characteristics in a swirl chamber type diesel engine using CFD code. The smallest passage hole area and the smallest passage hole angle demonstrate rapid speed in the combustion process, but the combustion at the end of the compression process leans toward the left. The largest passage hole area and the greatest passage hole angle demonstrate themselves to have a slower combustion process than other cases. In the largest passage hole area, the heat release rate during the diffusion combustion process begins later, compared to the other cases, and the heat release period is shorter. The inclination angles are similar by comparison with the heat releases according to the passage hole inclination angles. It is believed that in the largest passage hole area, the insufficient amount of oxygen cannot combine with the nitrogen to form various oxides. In the case of the smallest passage hole area, it is believed that the flame propagation of the main combustion chamber is difficult because of the narrow passage hole; moreover, an excess of oxygen can combine with the nitrogen to form various oxides. In the smallest passage hole area, soot concentrations rapidly increase in the swirl chamber because of a lack of oxygen compared to the other cases.

Nomenclature

A	: Passage hole area
ATDC	: After top dead center
CA	: Crank angle
CR	: Compression ratio
D	: Diameter
VR	: Volume ratio (swirl chamber/main chamber)

Acknowledgments

This work was supported by a Grant-in-Aid for the Components and Materials Technology Development Programmers from the Korea Ministry of Commerce Industry and Energy (MOCIE) and the Centre for Automotive Parts Technology (CAPT) at Keimyung University, Daegu, Korea.

References

- [1] S. H. Choi and Y. T. Oh, Experimental study on emission characteristics and analysis by various oxygenated fuels in a D.I. diesel engine. *Int. J. Automotive Technology* 6 (3) (2005) 197-204.
- [2] D. P. Schmidt and M. L. Corradini, The internal flow of diesel fuel injector nozzles: a review, *Int. J. Engine Research*, 2 (1) (2001) 1-22.
- [3] M. P. Poonia, A. Ramesh and R. R. Gaur, Experimental investigation of the factors affecting the performance of a LPG - diesel dual fuel engine. *SAE paper No. 1999-01-1123*, (1999).
- [4] S. Kimura, O. Aoki, H. Ogawa and S. Muranaka, New Combustion Concept for Ultra-Clean and High-Efficiency Small DI Diesel Engines. *SAE paper 1999-01-3681*, (1999).
- [5] J. M. Desantes, J. V. Pastor and A. Doudon, Study of the steady flow produced by direct injection diesel engine intake ports. *Proc. Instn Mech. Engrs, Part D: J. Automobile Engineering*, 215 (2001) 285-298.
- [6] K. Cunningham, R. K. Kee and R. G. Kenny, Reed valve modelling in a computational fluid dynamics simulation of the two-stroke engine, *Proc. Instn Mech. Engrs, Part A: J. Power and Energy*. 213 (1991) 37-45.
- [7] J. K. Yeom and H. Fujimoto, A study on the behavior characteristics of diesel spray by using a high pressure injection system with common rail apparatus. *KSME International Journal*, 17 (2003) 1371-1379.
- [8] M. A. Patterson, S. C. Kong, G. J. Hampson and R. D. Reitz, Modelling the effects of fuel injection characteristics on diesel engine soot and NO_x emissions. *SAE Paper 940523* (1994).
- [9] M. A. Patterson and R. D. Reitz, Model the effects of fuel spray characteristics on diesel engine combustion and emission. *SAE Paper 980131* (1998).
- [10] W. W. Pulkrabek, *Engineering Fundamentals of the Internal Combustion Engine Fundamentals*

- (Prentice Hall, New Jersey), (1999) 285-286.
- [11] H. Bensler, F. Buhren, E. Samson and L. Vervisch, 3-D CFD analysis of the combustion process in a DI diesel engine using a flamelet model. *SAE Paper* 2000-01-0662 (2000).
- [12] D. Jung and D. N. Assanis, Reduced quasi-dimensional combustion model of the direct injection diesel engine for performance and emissions predictions, *KSME International J.* 18 (2004) 865-876.
- [13] J. B. Heywood, *Internal Combustion Engine Fundamentals*, McGraw-Hill Book Company, New York, USA, (1988).
- [14] W. W. Pulkrabek, *Engineering Fundamentals of the Internal Combustion Engine*, Pearson Prentice Hall, New Jersey, USA, (2003).



Gyeong Ho Choi received his B.S. degree in Mechanical Engineering from Sungkyunkwan University, Korea, in 1986. He then obtained his M.S. and Ph.D. degrees in Mechanical Engineering from University of Alabama in 1988 and 1992, respectively. Dr. Choi is currently a Chairman of Board of Director at EROOM G&G, KOSDAQ Company, and a Advising Professor at King Mongkut's University of Technology North Bangkok in Thailand. He was a Professor at College of Automotive Engineering at Keimyung University from 1993 to 2008. His research interests include alternative energy in internal combustion engine, homogeneous charge compression ignition engine, and hybrid electric vehicle.



Yon Jong Chung received his B.S., M.S. and Ph.D. degrees in Mechanical Engineering from Sungkyunkwan University, Korea, in 1985, 1988 and 1991 respectively. Dr. Chung is currently a Professor at the Department of Automotive Engineering at Daegu Mirae College in Gyeongsan-si, Korea. He was a visiting scholar from 2007 to 2008 at the Plug-in Hybrid Electric Vehicle Research Center of UC Davis, USA. His research interests include combustion characteristics of engine, hybrid electric vehicle, and ultra low emission technology.



Yong Hoon Chang received his B.S. and M.S. degrees in Mechanical Engineering from Sungkyunkwan University, Korea, in 1989 and 1991 respectively. He then obtained his Ph.D. degree in Mechanical Engineering from University of Florida, USA, in 1997. Dr. Chang is currently a Professor at the Department of Mechanical & Automotive Engineering at Induk University in Seoul, Korea. His research interests include automatic control, hybrid electric vehicle, and automotive engine technology.



Sung Bin Han received his B.S. degree in Machine Design from Sungkyunkwan University, Korea, in 1984. He then obtained his M.S. and Ph.D. degrees in Mechanical Engineering from Sungkyunkwan University in 1986 and 1989, respectively. Dr. Han is currently a Professor at the Department of Mechanical & Automotive Engineering at Induk University in Seoul, Korea. He was a visiting scholar from 1996 to 1997 at the Sloan Automotive Lab of MIT, and from 2002 to 2003 at the Combustion Lab of UC Berkeley, USA, respectively. His research interests include combustion stability, homogeneous charge compression ignition engine, hybrid electric vehicle, and automotive engine technology.